JOURNAL OF CATALYSIS 108, 401–408 (1987)

Hydrodesulfurization over a TiO_2–ZrO_2-Supported CoO–MoO_3 Catalyst

F. P. DALY, H. ANDO, J. L. SCHMITT, AND E. A. STURM

American Cyanamid Company, Chemical Research Division, 1937 West Main Street, Stamford, Connecticut 06904

Received May 12, 1987; revised July 17, 1987

The binary oxide TiO_2–ZrO_2, whose chemical and physical properties were found to be strongly dependent on metal oxide ratio, precipitation methodology, and calcination temperature, was investigated as a support material for a CoO–MoO_3 hydrodesulfurization (HDS) catalyst. Thiophene HDS studies at 1 atm and 300°C revealed that the TiO_2–ZrO_2-supported catalyst had an initial activity, on a weight basis, over twice that of a CoO–MoO_3/Al_2O_3 catalyst, but suffered rapid deactivation. Nitric oxide chemisorption/temperature-programmed desorption (TPD) results suggest that the high initial activity of the TiO_2–ZrO_2-supported catalyst may be due to a weaker Mo–support interaction, yielding a greater number of more reactive coordinatively unsaturated Mo sites. Thermal gravimetric analysis and differential scanning calorimetry results suggest that deactivation of the TiO_2–ZrO_2-supported catalyst is at least in part due to coke formation. © 1987 Academic Press, Inc.

INTRODUCTION

Over the years a considerable amount of research has been devoted to studying the surface properties of the most effective hydrodesulfurization catalyst, CoO–MoO_3/Al_2O_3. This has included attempts to define the active catalyst species, the role of CoO, and the hydrodesulfurization reaction mechanism of model compounds. Another less-examined area is the role of the support.

The traditional view of a catalyst support has been that of an inert carrier for the catalytically active metal. Thereby, the support provided a surface for metal dispersion and enhanced thermal stability permitting continuous use at elevated temperatures. More recently, the physical and chemical properties of the support have been recognized as major contributors to resultant catalytic activity (*1*). While the physical properties of the support have been related to metal dispersion (*2*), the chemical properties have been related to both metal dispersion and electronic effects.

Yamazata *et al.* (*3*) have reported that molybdenum–support interaction is dependent on the number of anionic hydroxyl groups on the surface of the support. Muralidar *et al.* (*4*) have also reported that the concentration of anionic hydroxyl groups on the surface of a support affects molybdenum dispersion. Lercher and Noller (*5*) have shown by infrared studies a direct correlation between Brønsted acid strength of the hydroxyl bond on metal oxides and the Sanderson intermediate electronegativity of the metal oxide.

Recently, we reported (*6*) a correlation between nitric oxide chemisorption/TPD results and the calculated electronegativity of the support for a series of metal-oxide-supported MoO_3 catalysts. The results suggested that supports with calculated electronegativity values greater than Al_2O_3 yield more reactive sites, possibly due to a weaker Mo–support interaction.

As a consequence of these results we

0021-9517/87 $3.00
Copyright © 1987 by Academic Press, Inc.
All rights of reproduction in any form reserved.

investigated the use of binary oxides as supports for hydrodesulfurization catalysts. Our principle objective was to identify a support material that would promote HDS activity by enhancing the metal–support interaction while maintaining a high metal dispersion. This paper presents results for a series of TiO_2–ZrO_2-supported catalysts which suggest that variations in Mo–support interaction can affect catalyst activity for HDS.

EXPERIMENTAL

Sample Preparation

Samples of TiO_2–ZrO_2 were prepared by calcination of the hydroxides at 300 to 700°C for 3 h. The coprecipitated hydroxides were prepared in three ways: homogeneous precipitation using urea (*7*), direct addition of ammonium hydroxide, and hydrolysis of the metal alcoxides (*8*).

For the homogeneous precipitation procedure (HPP), an aqueous solution of $TiCl_4$, $ZrOCl_2$, and urea was heated to 95°C with constant stirring. Precipitation was complete after 2 to 3 h, at which time the pH of the solution was approximately 7. The precipitate was then filtered off, washed with deionized water to remove chloride ions, and dried overnight at 120°C (Table 1, Supports A–D).

The second method of precipitation involved the direct addition of concentrated ammonium hydroxide at a rate of approximately 5 cc/min to an aqueous solution (0.18 *M*) of $TiCl_4$ and $ZrOCl_2$. When the pH reached 8.5 the precipitate was filtered off, washed with deionized water, and dried overnight at 120°C (Table 1, Support E).

The third method of precipitation, hydrolysis of the metal alcoxides, namely, titanium(IV) butoxide and zirconium *n*-propoxide, was performed at room temperature in *n*-propanol (Table 1, Supports F and G). Hydroxides were precipitated from 10 wt% solutions using both a stoichiometric amount of water (Support G) and five times the stoichiometric amount (Support F) added dropwise at a rate of approximately 5 cc/min. The samples were then washed with *n*-propanol and dried at 120°C for 2 h.

The CoO–MoO_3 catalysts were prepared by impregnation of the TiO_2–ZrO_2 supports (40 × 80 mesh) using the incipient wetness technique. Supports were first impregnated with an aqueous solution of ammonium heptamolybdate, dried at 120°C, impregnated with an aqueous solution of cobalt nitrate, dried at 120°C, and calcined in flowing air at 350°C for one hour. Final composition, based on the concentration of the impregnation solutions, was 5 wt% CoO and 16 wt% MoO_3.

Nitric Oxide Chemisorption/TPD

NO chemisorption/TPD studies were performed in a flow apparatus equipped

TABLE 1

Description of TiO_2–ZrO_2 Support Materials

Support	Calcination temperature (°C)	Surface area (m^2/g)	NH_3 chemisorption (μmoles/g)	NH_3 chemisorption (μmoles/m^2)	Ti : Zr ratio Bulk	Ti : Zr ratio XPS
A	500	125	621	4.96	4 : 1	—
B	500	280	1014	3.62	1 : 1	—
C	500	90	722	8.02	1 : 4	—
D	350	367	1256	3.42	1 : 1	0.52 : 1
E	350	246	1207	4.91	1 : 1	0.44 : 1
F	350	287	736	2.56	1 : 1	0.83 : 1
G	350	254	1349	5.31	1 : 1	0.90 : 1

with a thermal conductivity detector and quadrupole mass spectrometer as previously described (*6*). All catalyst samples (250 mg) were presulfided *in situ* at 400°C for 1 h with 10 vol% H_2S in H_2 prior to NO chemisorption.

After saturation of the catalyst with NO the sample was heated in a helium stream (50 cc/min) to 400°C at a rate of 20°C/min. The composition of the effluent gas was measured at 1-min intervals using the on-line quadrupole mass spectrometer. The ratio of N_2O/NO was determined from the sum of the intensities of the N_2O and NO peaks.

Ammonia Chemisorption

Ammonia chemisorption measurements were made using the same apparatus described for NO chemisorption studies. Samples (250 mg) were first heated under a helium flow (50 cc/min) to 400°C for 1 hr. They were then cooled to 30°C and flushed with a 20 vol% NH_3 in helium stream for 30 min. Ammonia chemisorption values were obtained by measuring the amount of NH_3 desorbed on temperature programming from 30 to 400°C at a rate of 25°C/min using a thermal conductivity detector.

Hydrodesulfurization Activity

Catalyst samples were tested for initial thiophene hydrodesulfurization activity using a pulse-mode reactor at 300°C and 1 atm. The catalyst (0.05 cc) was presulfided at 400°C in 10 vol% H_2S in H_2 prior to testing. A 200-μl sample of 11 vol% thiophene in H_2 was injected into a H_2 stream (40 cc/min). Thiophene conversion was measured on-line using a gas chromatograph equipped with a flame ionization detector and a 3 ft × $\frac{1}{8}$ in. column packed with OV-17/Chromosorb Q.

Steady-state activity measurements were made with presulfided catalysts at 300°C and 1 atm in a fixed bed (0.5 cc), tubular reactor (*9*). As before, thiophene conversion was measured on-line using a gas chromatograph.

Hydrodesulfurization activity test results are reported as relative weight activity (RWA) and relative volume activity (RVA), with American Cyanamid's commercial TRILOBE (Trademark of American Cyanamid) HDS-20 catalyst (5 wt% CoO–16 wt% MoO_3/Al_2O_3) assigned RWA and RVA values of 100. These values are based on calculated rate constants assuming a psuedo-first-order reaction in thiophene.

Thermal Analysis

Thermal gravimetric analyses (TGA) were performed with a Perkin–Elmer TGS-2. Differential scanning calorimetry (DSC) experiments were performed with a Perkin-Elmer high-temperature DTA/DSC. For the TGA experiments, 7-mg samples were scanned from 45 to 1000°C at a rate of 25°C/min in an air flow of 40 cc/min. DSC experiments were performed under the same conditions using 28-mg samples.

RESULTS AND DISCUSSION

Wang *et al.* (*10*) have previously reported that the composition of TiO_2–ZrO_2 affects the resultant surface area and acidity. For samples calcined at 550°C, they reported a maximum surface area of 240 m^2/g at a $TiO_2:ZrO_2$ molar ratio of 1 : 1. As presented in Table 1 (Supports A–C) we observe a similar maxima of 280 m^2/g at a $TiO_2:ZrO_2$ molar ratio of 1 : 1 for samples prepared by HPP and calcined at 500°C. For this same molar ratio we also observed the highest NH_3 chemisorption value, 1010 μmoles/g, suggesting the highest acidity (*11*), in agreement with previous results (*10*).

In defining the effects of other preparation variables on surface area we examined the effect of calcination temperature. As illustrated in Fig. 1, we found that the calcination temperature has a strong effect on surface area. For two series of samples

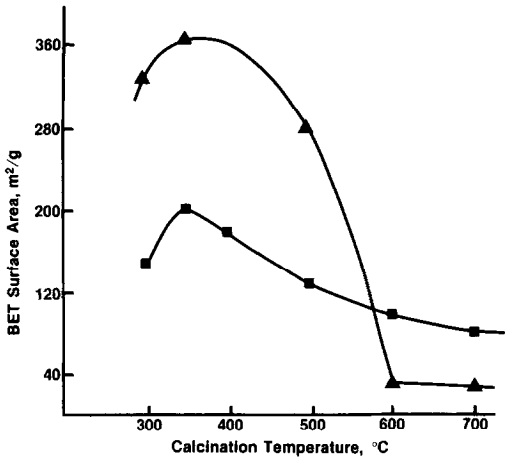

FIG. 1. Effect of calcination temperature on TiO_2–ZrO_2 N_2 BET surface area. (▲) $TiO_2:ZrO_2$ molar ratio of 1 : 1; (■) $TiO_2:ZrO_2$ molar ratio of 4 : 1.

prepared by HPP and with $TiO_2:ZrO_2$ molar ratios of 4 : 1 and 1 : 1, maximum surface areas were obtained at a calcination temperature of 350°C. The values were 208 and 367 m^2/g, respectively. XRD analyses revealed that for samples with a $TiO_2:ZrO_2$ molar ratio of 1 : 1, those calcined between 300 and 500°C were amorphous while those calcined at 600 and 700°C had intense crystalline patterns analogous to $ZrTiO_4$.

The effect of precipitation methodology on surface area was also investigated. For a series of samples calcined at 350°C, surface areas ranged from 246 to 367 m^2/g (Table 1, Supports D–G). The highest value was for Support D prepared by HPP. This is probably because the hydrosol is formed with a minimum of local hydroxide ion concentration gradients, which would occur upon direct addition of ammonium hydroxide (Support E) or water in the case of the alcogels (Supports F–G). This reduction in concentration gradients permits the growth of smaller crystals yielding a calcined material with a higher surface area.

Precipitation methodology was also found to affect acidity, as defined by NH_3 chemisorption. As presented in Table 1, NH_3 chemisorption values per unit surface area ranged from 2.56 to 5.31 $\mu moles/m^2$. A similar variation was also observed for Supports A–C with different $TiO_2:ZrO_2$ molar ratios suggesting that variations in the precipitation methodology could be affecting the surface chemistry of the samples. XPS analysis confirmed this by revealing that the Ti : Zr surface atom ratios (*12*) were different from the bulk molar ratio of 1 : 1 as presented in Table 1, even though product recoveries were approximately 95%.

Catalyst Activity

As a consequence of these results a series of TiO_2–ZrO_2-supported CoO–MoO_3 catalysts were prepared and evaluated by NO chemisorption/TPD. The results are presented in Table 2. In comparison to an Al_2O_3-supported CoO–MoO_3 catalyst a number of TiO_2–ZrO_2-supported catalysts exhibited higher NO chemisorption values and N_2O/NO TPD ratios.

Previously, we reported (*6*) that the reactivity of the Mo sites for the disproportionation of chemisorbed NO to N_2O, defined as the R_d value and equal to the ratio of the N_2O/NO TPD ratio to the level of NO chemisorbed, is related to the electronegativity of the support which affects the molybdenum–support interaction. The higher the support electronegativity, the weaker the metal–support interaction, the higher the R_d value, and, hence, the more reactive the Mo site. The NO chemisorption/TPD results for the CoO–MoO_3 cata-

TABLE 2

NO Chemisorption/TPD Results for CoO–MoO_3/TiO_2–ZrO_2 Catalysts

Catalyst	Support	NO chemisorption/TPD results			
		NO uptake		N_2O/NO ratio	$R_d(10^{-3})$
		(μmoles/g)	($\mu moles/m^2$)		
A	A	336	2.69	0.49	1.76
B	B	421	1.50	—	—
C	C	168	1.87	0.45	2.68
D	D	752	2.05	0.81	1.08
E	E	252	1.02	0.60	2.38
F	F	381	1.33	0.57	1.50
G	G	64	0.25	0.08	1.25
HDS-20	Al_2O_3	365	1.41	0.24	0.66

lysts made with TiO_2–ZrO_2 reveal higher R_d values in comparison to that obtained for an Al_2O_3-supported catalyst. This would suggest that the Mo sites are more reactive for NO disproportionation and that the Mo–support interaction is weaker than that for the Al_2O_3-supported catalyst. Furthermore, for Catalyst D the NO uptake on both a weight and surface area basis was significantly higher than that for the Al_2O_3-supported catalyst suggesting a higher concentration of coordinatively unsaturated Mo sites (*13*).

Jung *et al.* (*9*) reported a correlation between NO chemisorption and HDS activity for a series of MoO_3/Al_2O_3 catalysts of varying metal loading. Since NO chemisorption characterizes the initial state of the catalyst, both initial and steady-state activity measurements were made using pulse and continuous-flow reactors. The initial HDS RWA value of Catalyst D was 274, over twice that of the Al_2O_3-supported catalyst (RWA = 100). Since the density of the TiO_2–ZrO_2 support was 80% higher than that of the Al_2O_3 support the RVA value was also higher, 492 versus 100, respectively. However, the steady-state activity of Catalyst D was significantly lower with RWA and RVA values of 20 and 36, respectively.

Catalyst Deactivation

To define the cause of this rapid decrease in activity, TGA and DSC analyses using air were performed on catalysts prepared with both TiO_2–ZrO_2 (Catalyst D) and Al_2O_3 (HDS-20). The results are presented in Figs. 2 and 3. Figure 2 shows the TGA results of used and fresh samples of Catalyst D and HDS-20. These results reveal weight loses for the used samples of Catalyst D and HDS-20 at approximately 100, 300, 465, and 644°C. The only weight loss for the fresh sample of Catalyst D occurs at 100°C. DSC analyses (Fig. 3) reveal that the weight losses at 300, 465, and 644°C are a consequence of exothermic reactions.

The fact that both the fresh and used samples exhibit weight losses at 100°C suggests that these weight losses are due to absorbed water on the fresh catalyst and absorbed hydrocarbons on the used catalysts. Since only the used samples of Catalyst D and HDS-20 exhibit weight losses at 300°C and these samples were sulfided, it is believed these weight losses are due to the oxidation of the metal sulfides to metal oxides. The weight losses at 465 and 644°C for the used samples are attributed to two different forms of coke (*14*), an observation which has been previously reported for

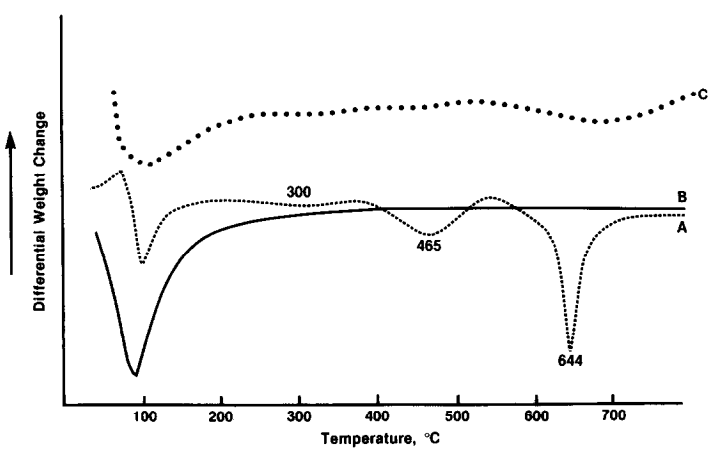

FIG. 2. Thermal gravimetric analyses of fresh and used catalysts. (A) Used MoO_3–CoO/TiO_2–ZrO_2; (B) fresh MoO_3–CoO/TiO_2–ZrO_2; (C) used MoO_3–CoO/Al_2O_3.

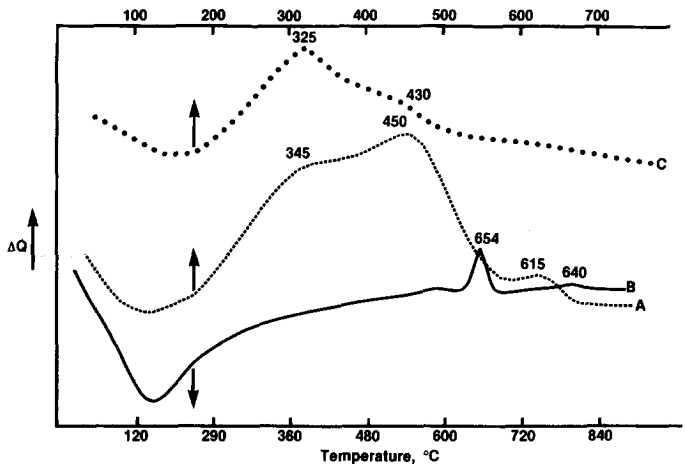

FIG. 3. Differential scanning calorimetry analyses of fresh and used catalysts. (A) Used MoO_3–CoO/TiO_2–ZrO_2; (B) fresh MoO_3–CoO/TiO_2–ZrO_2; (C) used MoO_3–CoO/Al_2O_3.

catalysts used in synthesis gas reactions (*15, 16*). The exotherm at 654°C on the DSC curve for a fresh sample of Catalyst D, for which there is no associative weight loss, is attributed to a phase change of the TiO_2–ZrO_2 support from amorphorous to crystalline as earlier XRD results revealed.

Assuming that the weight losses at 465 and 644°C are due to coke deposition, the levels of carbon on Catalyst D and HDS-20 are 12 and 6 wt%, respectively. The higher level of carbon on Catalyst D suggests that its rapid rate of deactivation may be due to a more rapid rate of coke formation.

Deactivation Mechanism

Kraus and Zdrazil (*17*) have reported that the principle thiophene HDS reaction mechanism over sulfided Co–Mo catalysts is as follows:

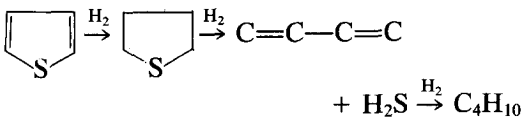

They also report the oligomerization of butadiene with the formation of C_8 and higher hydrocarbons.

As presented in Table 1, the NH_3 chemisorption value for the TiO_2–ZrO_2 used to prepare Catalyst D was 1256 μmoles/g. This value is 57% higher than that for the Al_2O_3 support used to prepare HDS-20 and suggests that Catlyst D is more acidic (*11*). In addition, Mikovsky and Silvestri (*18*) have reported that a CoO–MoO_3/TiO_2–ZrO_2 catalyst consumed 27% less hydrogen than an Al_2O_3-supported catalyst to achieve the same level of sulfur removal from a residuum oil. If the above reaction scheme is valid for Catalyst D, and a higher concentration of butadiene were to be formed, as Mikovsky and Silvestri results suggest, it is possible that butadiene could interact with the more acidic functionalities of TiO_2–ZrO_2 via a carbonium ion mechanism leading to olefin polymerization and more rapid coke formation.

Catalyst deactivation by coke formation can occur in two ways; surface coverage of active sites or pore plugging (*19*). Mercury pore size distribution (PSD) measurements revealed that the TiO_2–ZrO_2 materials made by HPP were microporous suggesting that the mode of deactivation may be pore plugging. As a consequence, a series of TiO_2–ZrO_2 (1 : 1) samples were prepared with different porosities as presented in Table 3. The thiophene HDS activity of CoO–MoO_3 catalyst prepared with these supports is presented in Table 4.

Using the data presented in Tables 3 and

TABLE 3

Physical Properties of TiO_2-ZrO_2 Support Materials

Support	BET surface area (m^2/g)	Mercury PSD results		
		Surface area (m^2/g)	Pore volume (cc/g)	Pore mode radius (Å)
D	367	33	0.122	20
H	312	193	0.308	22
I	177	136	0.299	33
J	128	125	0.274	30

4, a direct relationship between support porosity and catalyst stability has been found. As illustrated in Fig. 4, the percentage difference in steady-state versus initial HDS activity (x axis) decreases as the ratio of the surface area derived from mercury PSD (pore radii > 20 Å) versus the BET surface area (y axis) increases. These results show that as the porosity of the support increases, yielding fewer pores <20 Å, the rate of catalyst deactivation, measured by the difference in initial versus steady-state activity, decreases. This by itself would suggest that catalyst deactivation is due to pore plugging. However, since the Hg PSD and N_2 BET surface areas of Catalyst J are comparable, but the steady-state activity is 43% less than the initial activity, it also appears that surface coverage of active sites may also be occurring.

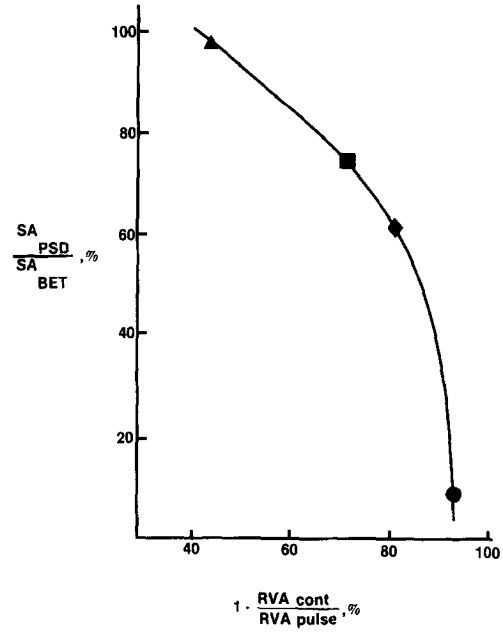

FIG. 4. Effect of TiO_2-ZrO_2 porosity on catalyst stability. (●) Catalyst D; (♦) Catalyst H; (■) Catalyst I; (▲) Catalyst J.

CONCLUSION

The results presented strongly suggest that the preparation methodology for TiO_2-ZrO_2 not only affects its physical properties such as surface area and porosity, but also its surface chemistry. In the case of TiO_2-ZrO_2-supported catalyst, such changes in surface chemistry can alter the strength of the Mo–support interaction which can affect the concentration and reactivity of coordinatively unsaturated Mo sites active for HDS.

TABLE 4

Thiophene Hydrodesulfurization Activity Test Results for $CoO-MoO_3/TiO_2-ZrO_2$ Catalysts

Catalyst	Support	HDS activity test results, RWA/RVA	
		Initial	Steady state
D	D	274/492	20/36
H	H	152/286	32/55
I	I	74/130	22/38
J	J	63/107	36/61

ACKNOWLEDGMENTS

The authors thank Ms. R. Ferrillo and Dr. J. Brinen of the Chemical Research Scientific Services Department for their assistance in thermal analysis and XPS studies, respectively.

REFERENCES

1. Acrea, G. J. K., Bird, A. J., Jenkins, J. W., and King, F., "Catalysis" (C. Kemball and D. A. Dowden, Eds.), Vol. 1, p. 4. The Royal Society of Chemistry, 1981.
2. Moss, R. L., "Experimental Methods in Catalytic Research" (R. B. Anderson and P. T. Dawson, Eds.), Vol. 2, p. 44. Academic Press, New York, 1976.
3. Yamazata, N., Owada, Y., Okayabi, S., and Tanabe, K., *J. Catal.* **47**, 358 (1977).
4. Muralidar, G., Massoth, F. E., and Shabtai, J.,

Amer. Chem. Soc. Div. Petrol. Chem. Prepr. **27**(3), 722 (1982).

5. Lercher, J. A., and Noller, H., *J. Catal.* **77**, 15 (1982).
6. Daly, F. P., Schmitt, J. L., and Sturm, E. A., *J. Catal.* **97**, 248 (1986).
7. Willard, H. H., and Tang, N. K., *J. Amer. Chem. Soc.* **59**, 1190 (1937).
8. Teichner, S. J., Nicolson, G. A., Vicarini, M. A., and Gardes, G. E. E., *Adv. Coll. Interf. Sci.* **5**, 245 (1976).
9. Jung, H. J., Schmitt, J. L., and Ando, H., "Proceedings, 4th Int. Conf. in the Chemistry and Uses of Molybdenum." Golden, CO, 1982.
10. Wang, I., Chang, W. F., Shiau, R. J., Wu, J. C., and Chung, C. S., *J. Catal.* **83**, 428 (1983).
11. Webb, A. N., *Ind. Eng. Chem.* **49**, 261 (1957).
12. Daly, F. P., Brinen, J. S., and Schmitt, J. L., *Appl. Catal.* **11**, 161 (1984).
13. Millman, W. S., and Hall, W. K., *J. Catal.* **60**, 404 (1979).
14. Buyanov, R. A., *Kinet. Catal.* **21**(1), 189 (1980).
15. Daly, F. P., *J. Catal.* **89**, 131 (1984).
16. McCarty, J. G., and Wise, H. J., *J. Catal.* **57**, 406 (1979).
17. Kraus, J., and Zdrazil, M., *React. Kinet. Catal. Lett.* **6**, 475 (1977).
18. Mikovsky, R. J., and Silvestri, A. J., U.S. Patent 4,128,505 (1978).
19. El-Kady, F. Y. A., and Mann, R., *J. Catal.* **69**, 147 (1981).